Individual and combined effects of ph and lactic acid concentration on Listeria innocua inactivation: development of a predictive model and assessment of experimental variability

Janssen, M.H.M.; Geeraerd, A.H.; Cappuyns, A.; Garcia-Gonzalez, L.; Schockaert, G.; Van Houteghem, N.; Vereecken, K.M.; Debevere, J.; Devlieghere, F.; Van Impe, J.F.

published in
Applied and Environmental Microbiology
2007

DOI (link to publisher)
10.1128/AEM.02198-06

document version
Publisher's PDF, also known as Version of record

Applied and Environmental Microbiology, Mar. 2007, p. 1601–1611 Vol. 73, No. 5
0099-2240/07/$08.00+0 doi:10.1128/AEM.02198-06

Individual and Combined Effects of pH and Lactic Acid Concentration on *Listeria innocua* Inactivation: Development of a Predictive Model and Assessment of Experimental Variability▽

M. Janssen,[1] A. H. Geeraerd,[2] A. Cappuyns,[1] L. Garcia-Gonzalez,[1] G. Schockaert,[1] N. Van Houteghem,[3] K. M. Vereecken,[1]† J. Debevere,[3] F. Devlieghere,[3] and J. F. Van Impe[1]*

Division of Chemical and Biochemical Process Technology and Control, Department of Chemical Engineering, Katholieke Universiteit Leuven, W. de Croylaan 46, B-3001 Leuven, Belgium[1]; Division of Mechatronics, Biostatistics and Sensors (MeBioS), Department of Biosystems (BIOSYST), Katholieke Universiteit Leuven, W. de Croylaan 42, B-3001 Leuven, Belgium[2]; and Laboratory of Food Microbiology and Food Preservation, Department of Food Safety and Food Quality, Ghent University, Coupure Links 653, B-9000 Ghent, Belgium[3]

Received 19 September 2006/Accepted 22 December 2006

In food technology, organic acids (e.g., lactic acid, acetic acid, and citric acid) are popular preservatives. The purpose of this study was to separate the individual effects of the influencing factors pH and undissociated lactic acid on *Listeria innocua* inactivation. Therefore, the inactivation process was investigated under controlled, initial conditions of pH (pH_0) and undissociated lactic acid ($[LaH]_0$). The resulting inactivation curves consisted of a (sometimes negligible) shoulder period followed by a descent phase. In a few cases, a tailing phase was observed. Depending on the conditions, the descent phase contained one or two log-linear parts or had a convex or concave shape. In addition, the inactivation process was characterized by a certain variability, dependent on the severity of the conditions. Furthermore, in the neighborhood of the growth/no growth interface sometimes contradictory observations occurred. Overall, the individual effects of the influencing factors pH and undissociated lactic acid could clearly be distinguished and were also apparent based on fluorescence microscopy. Appropriate model types were developed and enabled prediction of which conditions of pH_0 and $[LaH]_0$ are necessary to obtain a predetermined inactivation (number of decimal reductions) within a predetermined time range.

Favored by their activity against a broad spectrum of pathogenic and spoilage microorganisms, even at low concentrations, organic acids (e.g., lactic acid, acetic acid, and citric acid) are popular preservatives in the food industry, where a tendency towards minimal processing is observed. In addition, lactic acid bacteria are used in food production processes to produce fermented foods. Secondary to the fermentative effect, the lactic acid metabolism has a preservative effect due to the production of other antimicrobial substances such as hydrogen peroxide and organic acids (34).

The organic acid antimicrobial activity is twofold: (i) release of protons at dissociation lowers the extracellular pH, and (ii) the undissociated form of the acid is able to diffuse into the cell, affecting the cell metabolism. The latter effect is reported to result in a global inhibition due to acidification of the cytoplasm and a more specific inhibition of several metabolic and anabolic functions (1, 23, 35). The said antimicrobial activity can reveal itself in (i) inhibition, i.e., an early induction of the stationary phase, and (afterwards) (ii) inactivation, i.e., a decrease in cell concentration to values below the detection limit of the so-called target (pathogenic or spoilage) organism.

In predictive microbiology, the knowledge of microbial growth or death responses to environmental factors is translated into mathematical equations that enable prediction of microbial proliferation or inactivation in foods. Final application lies in the quantitative assessment of the microbial safety and quality of food products, e.g., in defining the critical control points within a hazard analysis and critical control point framework, in shelf-life studies (27), or in the exposure assessment step within microbiological risk assessments. Some models had already been developed to describe the influence of organic acids such as lactic acid on the evolution of the target organism, not only in pure culture but also in coculture with a lactic acid bacterium (19, 21, 22, 31, 40, 46). However, the individual effects of the factors undissociated lactic acid [LaH] and pH are still insufficiently quantified, especially for inactivation processes. To the best of the authors' knowledge, in only one study (9) was a model developed that describes the inactivation of *Listeria monocytogenes* as a function of pH and undissociated lactic or acetic acid. The differentiated effects of pH and undissociated acid were expressed as influencing t_{4D}, the time to a four-decimal-reduction inactivation (99.99%), and, unfortunately, no predictions of cell concentration at any time instance before or after t_{4D} could be made.

This study investigated the inactivation of *L. innocua* at controlled conditions of pH and [LaH]. The experimental

* Corresponding author. Mailing address: Department of Chemical Engineering, W. de Croylaan 46, B-3001 Leuven, Belgium. Phone: 32 16 321466. Fax: 32 16 322991. E-mail: jan.vanimpe@cit.kuleuven.be.
† Present address: Federal Agency for the Safety of the Food Chain, WTC III, Simon Bolivarlaan 30, B-1000 Brussels, Belgium.
▽ Published ahead of print on 5 January 2007.

setup was constructed to enable us to separate the effects of pH and [LaH], in contrast to several previous studies (19, 46) where pH and [LaH] had a one-to-one relationship defined by the buffer capacity of the medium.

MATERIALS AND METHODS

Strain and culture preparation. The *Listeria innocua* strain ATCC 33090 was used. Stock cultures were stored in glycerol (Acros) at a temperature of −80°C. For preculturing, 0.1 ml of this stock culture was added to 5 ml preculture medium (modified brain heart infusion [BHI] medium, see below) and incubated for 24 h at 30°C. After two 1-to-10 dilutions, 1 ml was added to 100 ml preculture medium and the mixture was incubated for 16 h at 30°C. Before inoculation, the cell suspension was centrifuged (10 min, 3,000 rpm, 22°C) (Eppendorf centrifuge 5810R). The supernatant was removed, and cells were washed with peptone water (8.5 g/liter NaCl [Acros], 1 g/liter peptone [Oxoid]). After a second centrifugation, cells were suspended in 20 ml of the experimental medium and inoculated.

Because of the observed variability for some of the experimental conditions (explained later in this text), replicate experiments were performed in parallel (i.e., at the same time). To avoid the possible influence of differences in preculturing conditions of inocula for these experiments, precultures were prepared as described above. However, before the first centrifugation step, precultures for parallel experiments were mixed and again separated into two parts, assuming identical inocula were obtained. Thereafter, the preculture treatment proceeded as described above.

Experimental conditions. Inactivation experiments were performed in 1-liter Erlenmeyer flasks (Duran Schott) provided with a side arm. Both openings (upper and side arm) were closed with screw caps containing a rubber septum. The Erlenmeyer flask was filled with 550 ml of a rich, modified brain heart infusion medium containing BHI (37 g/liter; Oxoid) supplemented with yeast extract (4 g/liter; Oxoid), glucose (18 g/liter; VEL), Tween 80 (1 ml/liter; Merck), $MgSO_4 \cdot 7H_2O$ (0.2 g/liter; Acros), and $MnSO_4 \cdot H_2O$ (0.04 g/liter; Acros). Before inoculation, the medium was flushed with N_2 to create an anaerobic atmosphere. The tested combinations of pH_0 and $[LaH]_0$ are graphically presented in Fig. 1. Conditions for which parallel experiments with mixed inoculum were performed are indicated in a box. A combination of initial pH (i.e., pH_0) and initial concentration of undissociated lactic acid (i.e., $[LaH]_0$) was set as follows. For clarity, the procedure is illustrated for setting $pH_0 = 3.5$ and $[LaH]_0 = 0.05$ M, as indicated by the thick box in Fig. 1. First, the pH of the medium was adjusted to a certain so-called "pH*" by the addition of the appropriate volumes of HCl (1 N; Acros) or KOH (0.10 g/liter; Acros). For the example, pH* equaled 3.99 (Fig. 1). In the second step, L(+)-lactic acid (Acros) was added. By preliminary experiments, it was ensured that the effective concentration of lactic acid was not dependent on poly-lactic acid formation. Because of its high viscosity, measurements of weight of lactic acid were more accurate than volumetric measurements. Therefore, for most of the experiments, the mass of lactic acid necessary to reach the appropriate initial concentration of total lactic acid (i.e., $LaH_{tot,0}$; initial sum of both the dissociated and undissociated forms) was added ($LaH_{tot,0} = 0.0718$ M in the example). As a consequence, the pH of the medium decreases from pH* on (according to the lower titration curve indicated in Fig. 1). If the resulting pH (3.37 in the example) was slightly different from the desired pH_0 (e.g., 3.5) a second pH adjustment was performed, reaching the desired conditions ($pH_0 = 3.5$ and $[LaH]_0 = 0.05$ M in the example). No extra buffers were added. Approximately 15 h before inoculation, flasks were placed on a rotary shaker (130 rpm; Heidolph Unimax 2010) in a cooling incubator at 12°C (cooling incubator series 6000; Termaks). *Listeria innocua* was inoculated at a concentration of approximately 10^8 CFU/ml. During the experiment, temperature was maintained at 12°C to ensure a possible coupling with microbial growth models recently developed by our research group (45, 46).

As indicated in detail in Fig. 1, 30 pH_0-$[LaH]_0$ combinations were tested, of which 11 had an initial undissociated lactic acid concentration ranging from 0.01 to 0.075 M (pH_0 ranging from 4.38 to 3.65) for a pH* equal to 6.20; 19 (pH_0-$[LaH]_0$) combinations were situated on other titration curves with a different starting pH (pH*) and formed an approximately rectangular shape in the pH-[LaH] plane (pH_0 ranging from 3.43 to 4.5 and $[LaH]_0$ ranging from 0 to 0.05 M). As such, the individual effect of, for example, pH_0 could be investigated at combinations with equal $[LaH]_0$. Similar to studies by Le Marc et al. (21) and Presser et al. (31), a value of 3.86 was chosen for the pK_a of lactic acid. The same pK_a value for all conditions was used, and thus, possible variation of the latter with increasing ionic strength (at high pH_0 and high $LaH_{tot,0}$) was ignored. This was based upon a study of Thylin et al. (42). It should be noted that this viewpoint is not followed by a recent study (7) in which the survival of *Escherichia coli* was observed to be influenced by ionic strength.

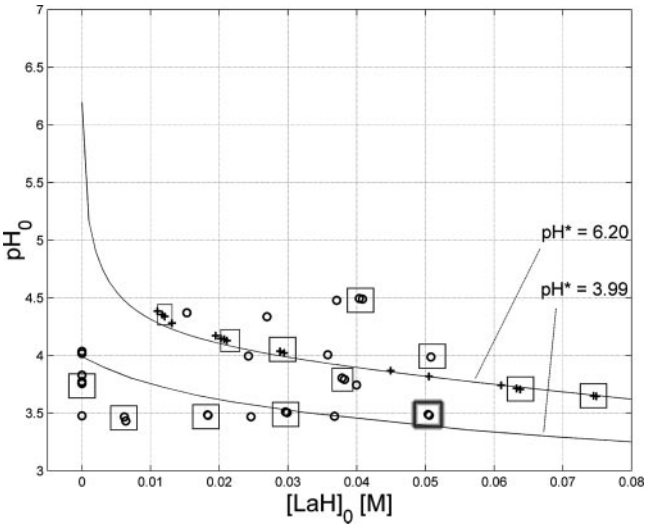

FIG. 1. Overview of the 30 pH_0-$[LaH]_0$ combinations tested. Eleven of these combinations were situated on the titration curve with pH* = 6.20 (+), and 19 formed a more or less rectangular shape (○). Condition symbols surrounded by a box correspond to experiments performed in parallel. The experiments with pH_0-$[LaH]_0$ combinations equal to 4.0 for pH_0 and 0 M for $[LaH]_0$ were performed in duplicate (4.13 and 0.0210 M, respectively) threefold, and the experimental condition (3.75 and 0 M, respectively) was investigated fourfold.

Measurements. At regular time intervals, samples (6 ml) were taken with a sterile syringe (Discardit II; Becton Dickinson) and needle (Microlance 3; Becton Dickinson) through the side septum. Cell concentration was determined by plating a dilution series of 1 ml of the sample (in peptone water) by means of a spiral plater (Eddy Jet, D-mode; IUL Instruments) on a selective medium based on the modified BHI medium, supplemented with LiCl (5 g/liter; UCB) and agar (18 g/liter; Oxoid). LiCl was added to enable possible future comparison with coculture experiments, as described by Vereecken et al. (45). Plates were incubated at 37°C for 24 to 48 h for samples at the end of the inactivation process. The remaining 5 ml of the sample was filtered over a membrane filter (Filtropur S 0.2; Sarstedt) to remove the cells. The pH of the supernatant was determined with a pH sensor (inoLab level 1; WTW) (accuracy of ±0.005 as stated by the producer). The lactic acid concentration in the sample was measured by gas chromatographic determination of the methyl ester. In sequential order, 0.1 ml β-hydroxybutyric acid (Merck Schuchardt) (internal standard), 1 ml H_2SO_4 (50%; Fisher Scientific), and 4 ml methanol (Acros) were added to 1.9 ml of the filtrate. Next, the mixture was heated to 55°C for 30 min. Afterwards, 2 ml distilled water and 1 ml chloroform (Acros) were added, and the mixture was shaken for 2 min. After separation of the aqueous and chloroform phases, 5 μl of the chloroform phase was injected into the gas chromatograph (Finnigan Trace GC Ultra), equipped with a flame ionization detector. Separation occurred on a 2-m column with 10% Carbowax 20 M on Chromosorb W-AW 80/100 (settings: gas flow, mobile phase [N_2], 40 ml/min; detection [H_2 plus air], 25 ml/min; temperature of column, 120°C; temperature of injection block, 240°C; and temperature of detection block, 245°C). By means of a calibration curve, peak factors equal to the ratio of the peak surface for lactic acid and the peak surface for β-hydroxybutyric acid were related to the lactic acid concentration in the sample. For the lactic acid measurements, a standard error of $8.420 \cdot 10^{-3}$ was obtained when the measured and calculated (based on mass of lactic acid added) $LaH_{tot,0}$ values were compared. The glucose concentration was determined with an enzymatic probe (Granutest; Merck).

For the experiments performed in duplicate and situated on the titration curves with pH* different from 6.20 (Fig. 1), the behavior of the cells during the exposure to adverse conditions was monitored. At regular time instances, a sample was inspected by oil immersion phase-contrast microscopy with an Olympus BX51 (objective, Ach 100×/1.25 oil [pH 3]; Olympus, Japan) to detect the formation of cell aggregates and their amount and morphology.

In addition, for an initial pH of 3.75, the effect of an increasing initial con-

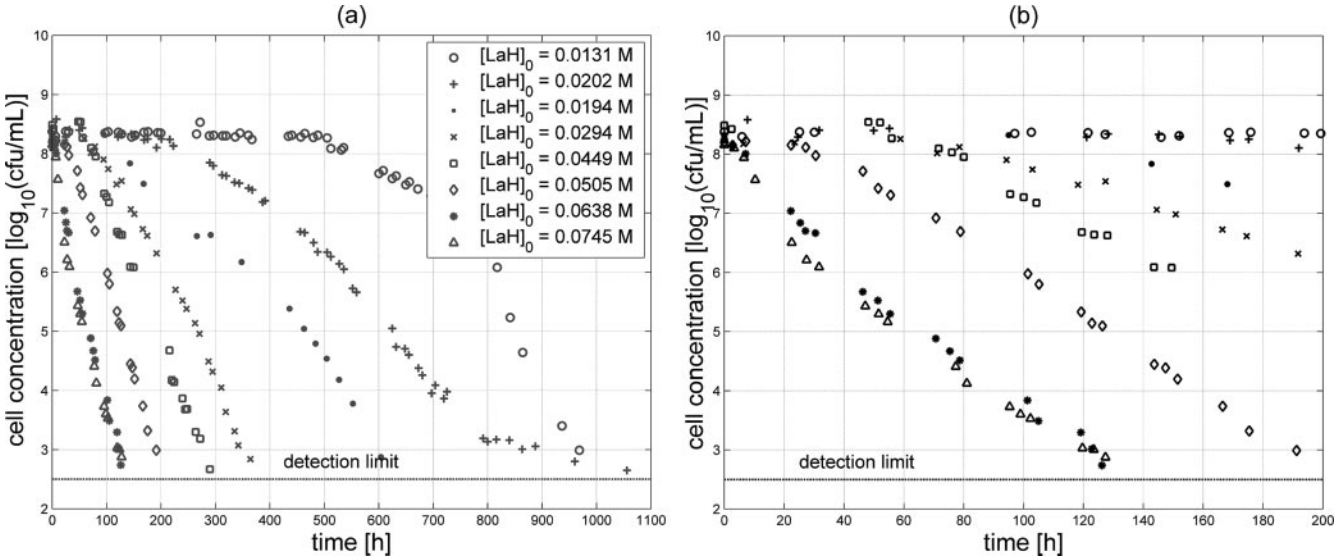

FIG. 2. *L. innocua* inactivation at pH_0-$[LaH]_0$ combinations on the titration curve with pH* equal to 6.20 for the full-time range (a) and a detailed view for time zero to 200 h (b).

centration of undissociated lactic acid (0 M, 0.0400 M, and 0.0610 M) was investigated through fluorescence microscopy. Cells were stained with carboxyfluorescein diacetate (cFDA; 1 mM in acetone [Molecular Probes, Leiden, The Netherlands]) and propidium iodide (PI; 2 mM in water [Molecular Probes]). A sample representing each experimental condition at viable cell concentrations of 10^4 (0 M), 10^5 (0.0400 M), and 10^6 (0.0610 M) CFU/ml was investigated. For this purpose, 100 μl of cell suspension was centrifuged (10 min at 4,660 × *g*; Biofuge pico [Heraeus Instruments, Brussels, Belgium]) and washed with phosphate-buffered saline (PBS; 50 mM, pH 7.2, consisting of 5.675 g/liter Na_2HPO_4 and 1.36 g/liter KH_2PO_4) for two times. Next, 1 μl of cFDA and 1.5 μl of PI were added to 100 μl of cell suspension in PBS. After incubation for 10 to 15 min in the dark at room temperature, samples were placed on ice. For each sample, five fluorescence images were taken with a Carl Zeiss Axio Imager A.1 (objective; Zeiss EC Plan-Neofluar, 100×/1.3 oil, pH 3; camera, Zeiss AxioCam MRm) and analyzed with an AxioVision LE V4.4 (Carl Zeiss Vision GmbH).

Modeling. Quantification of the individual effects of the concentration of undissociated lactic acid ($[LaH]_0$) and the pH (pH_0) was performed in two steps. First, a primary model suitable to describe the observed inactivation curves was selected. Second, variation of the primary model parameters with $[LaH]_0$ and pH_0 was translated into a polynomial or double-exponential expression.

(i) Determination of primary inactivation kinetics. For the modeling of the experimental data, GInaFiT (version 1.4), a freeware add-in for Microsoft Excel, was used (14). This software tool can calibrate the following models to the experimental data: (i) the traditional log-linear model (e.g., see reference 3), (ii) the log-linear model with shoulder and/or tail (13), (iii) Weibull-type models (2, 24), and (iv) a biphasic model (10) and a newly proposed biphasic model with a preceding shoulder period (14). Next to the parameter values, the tool also computes statistical measures such as the sum of squared errors (SSE), the mean sum of squared errors (MSE), and the root mean sum of squared errors (RMSE). The last criterion is useful in assessing whether a given model (linear or nonlinear) truly fits the data well, namely, its magnitude should be similar to the magnitude of the experimental error (33).

(ii) Secondary model describing the separate effects of $[LaH]_0$ and pH_0. The (individual) effects of $[LaH]_0$ and pH_0 on the microbial inactivation curves could be translated into the variation of the primary model parameters as a function of both factors. As will be shown in Results, the Weibull (or Weibull-type) model was selected as a primary model. The model equation can be written as follows, where t (h) is time, $N(t)$ (CFU/ml) is the cell concentration as a function of time, N_0 (CFU/ml) is the initial cell concentration, δ (h) is the time of the first log reduction, p (−) is the shape factor, $p > 1$ is a convex shape, $p < 1$ is a concave shape, and $p = 1$ is a log-linear shape (24):

$$N(t) = N_0 \cdot 10^{\left(-\left(\frac{t}{\delta}\right)^p\right)} \quad (1)$$

For the data with a residual cell concentration, N_{res}, the adapted Weibull model of Albert and Mafart (2) was used to obtain a good estimation for p and δ.

A secondary model for the variation of the Weibull parameters p and δ as a function of $[LaH]_0$ and pH_0 was developed. To facilitate the parameter estimation procedure, the $[LaH]_0$ and pH_0 data were centered around 0 and rescaled by subtracting their mean value ($\overline{[LaH]}_0 = 2.828 \times 10^{-2}$, $\overline{pH}_0 = 3.89$) and dividing by their standard deviation ($s_{[LaH]_0} = 2.113 \times 10^{-2}$ and $s_{pH_0} = 3.252 \times 10^{-1}$) (28). A second-order polynomial model was proposed for the variation of ln(δ) with the centered and scaled $[LaH]_0$ and pH_0 values. Partial F tests were used to find significant terms. Prediction of δ (that is, the original, untransformed values) was obtained by taking the antilogarithm of the fitted values, and a correction term for bias was included (26).

For p, a more complex model structure similar to the modified Gompertz equation for microbial growth described by Zwietering et al. (50) or the switching function applied by Van Impe et al. (43) was proposed.

The 95% confidence intervals for the secondary model parameters were calculated based on the variance-covariance matrix as, for example, described by Van Impe and coworkers (44).

For the processing of the experimental data and the parameter estimations for the secondary model, Matlab (version 6.1 R12; The MathWorks Inc., Natick, MA) was used.

RESULTS

Inactivation at pH_0-$[LaH]_0$ combinations on the titration curve with pH* equal to 6.20. Part of the resulting inactivation curves of the 11 (pH_0-$[LaH]_0$ combinations tested with pH* equal to 6.20 are illustrated in Fig. 2a. Inactivation at other (intermediary) lactic acid concentrations showed a similar behavior. From Fig. 2a, it can be concluded that by increasing $[LaH]_0$ and decreasing pH_0, the length of the shoulder period was reduced, while the inactivation rate increased.

In the evolution of the cell concentration as a function of time, two phases could be distinguished: (i) a period (e.g., ±500 h for $[LaH]_0 = 0.0131$ M) with a constant cell concentration (i.e., a shoulder period) followed by (ii) a period in which the cell concentration decreased to values below the detection limit (i.e., the descent phase). Depending on the combined pH_0-$[LaH]_0$ conditions, the latter phase consisted of

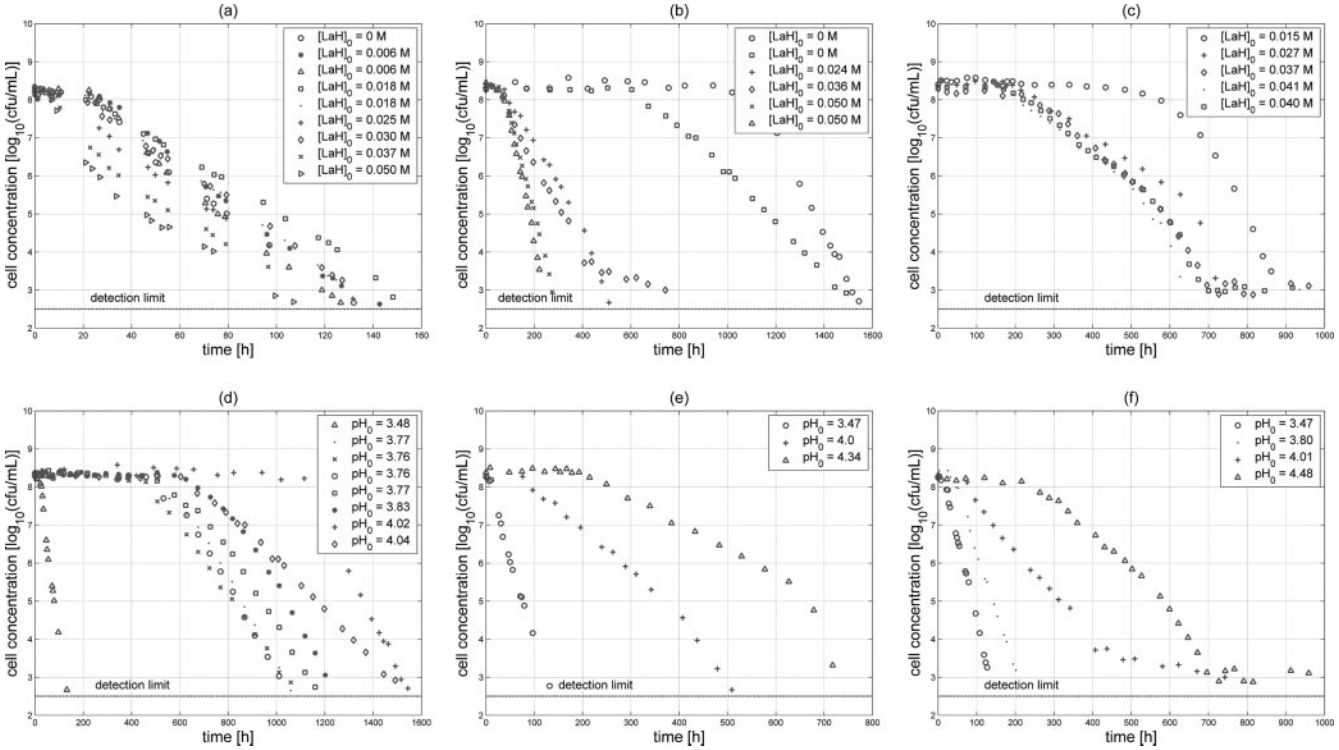

FIG. 3. Inactivation of *L. innocua* at pH_0-$[LaH]_0$ combinations situated in the rectangular shape. (Top) Influence of $[LaH]_0$ at pH_0 values of ±3.5 (a), 4.0 (b), and 4.5 (c). (Bottom) Influence of pH_0 at $[LaH]_0$ values of 0 M (d), ±0.025 M (e), and ±0.037 M (f).

one ($[LaH]_0$ = 0.0449 and 0.0505 M) or two ($[LaH]_0$ = 0.0131, 0.0202, 0.0194, and 0.0294 M) log-linear parts with respective slopes. Only the inactivation at $[LaH]_0$ equal to 0.0202 M showed a residual cell concentration (i.e., a tail). In addition, it has to be mentioned that at initial undissociated lactic acid concentrations of 0.0131 and 0.0202 M, inactivation rather followed a convex curve instead of a straight log-linear line. For $[LaH]_0$ above 0.063 M, the inactivation curve took a rather concave shape, which can be clearly seen on the close-up of the range from time zero to 200 h (Fig. 2b). During the experiments, the glucose concentration remained constant (data not shown), indicating that nutrient depletion cannot be the cause of the inactivation. As anaerobic conditions prevent *L. innocua* from producing acetic acid next to lactic acid (if any production would occur at all, given the inactivation of the microbe) (20), the prevailing lactic acid and pH conditions were the only explanatory factors for the observed inactivation process. Measurements of pH and lactic acid concentration (not shown) sometimes showed a slight increase for both. For 17.5% of the experiments, the increase in total lactic acid was higher than 0.01 M and combined with a pH increase of 0.2. These experiments also showed a long shoulder period (>380 h). A total of 17.5% of the experiments showed no change of lactic acid concentration or pH. These corresponded to severe conditions ($[LaH]_0$ = 0.0638 and 0.0749 M). The majority of the experiments (59%) had an almost constant lactic acid concentration, with a pH increase lower than 0.2 and a shoulder period shorter than 200 h. Only 6% of the experiments were characterized by a slight decrease in lactic acid concentration and a pH increase of less than 0.2. This could have an influence on the further evolution of the inactivation process and would suggest taking these rather dynamic profiles into account. However, the considered profiles could be a consequence of the effect of the initial pH and lactic acid concentration. Because a high increase in total lactic acid and pH was observed for experiments with a long shoulder period (inactivation at less severe conditions), the lactic acid likely is produced during maintenance of the microbial cells. As *L. innocua* is a neutrophilic microorganism, it tries to keep its intracellular pH at near-constant values when the extracellular pH decreases (16, 37, 39). As a result, and due to cell lysis when the cytoplasm comes into the extracellular environment, the environmental pH increases. Therefore, similar to several studies concerning the influence of pH and lactic acid on the growth of microorganisms (21, 31), the inactivation curves were evaluated against their initial pH and initial concentration of undissociated lactic acid.

Inactivation at pH_0-$[LaH]_0$ combinations forming a ± rectangular shape. The resulting inactivation curves for 18 of the 19 pH_0-$[LaH]_0$ combinations tested are presented in Fig. 3. The inactivation curves showed also a (sometimes almost negligible) shoulder period followed by a decrease of the cell concentration to values below the detection limit. The inactivation curves with $[LaH]_0$ within 0.0370 to 0.040 M (Fig. 3c) or pH_0 equal to 4.01 or 4.48 (Fig. 3f) showed a tail-like behavior. The cell concentration decreased slowly to values below the detection limit. Again, depending on the conditions, the descent phase consisted of one or two log-linear parts with the respective slopes.

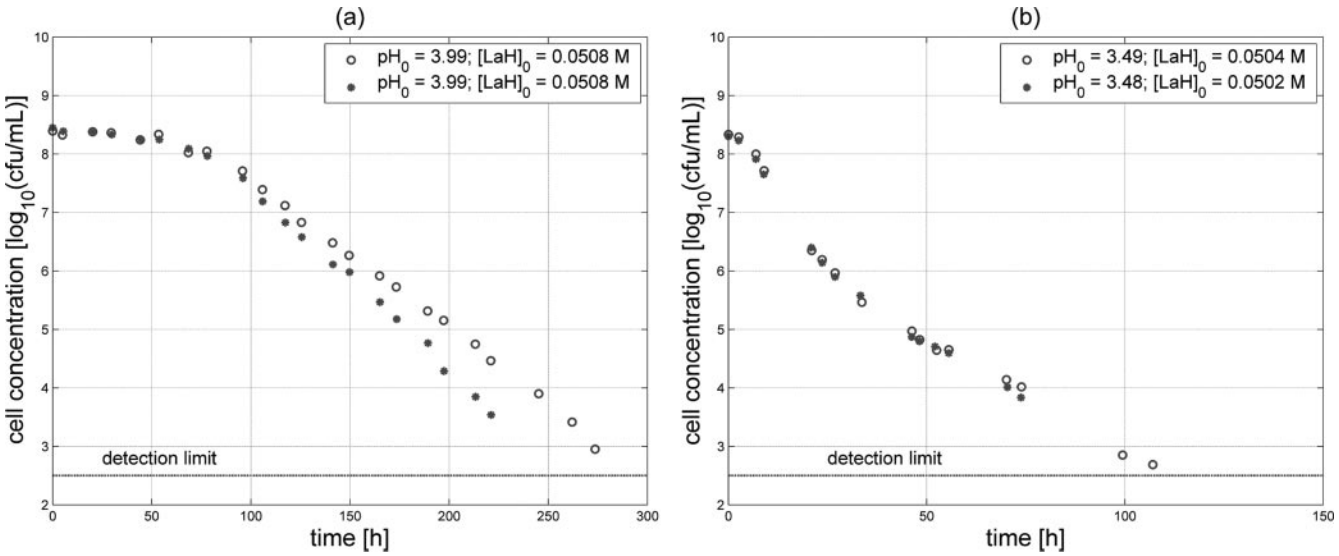

FIG. 4. Variation in inactivation for (almost) identical pH_0-$[LaH]_0$ conditions.

Regarding the inactivation curves at equal initial pH (Fig. 3, top) and equal initial undissociated lactic acid concentration (Fig. 3, bottom), the individual effects of $[LaH]_0$ and pH_0, respectively, could be derived. For the effect of $[LaH]_0$, it can be concluded that with variation of $[LaH]_0$, the length of the shoulder period changed, next to the change of the slope of the descent phase (see Fig. 3, top). The influence of $[LaH]_0$ was more pronounced at higher pH_0, as the combination of pH_0 equal to 4.5 and $[LaH]_0$ equal to 0 M resulted in growth of the microorganism (not shown). For each value of pH_0 tested in these experiments, there seemed to exist a concentration of lactic acid above which the length of the shoulder period remained constant: e.g., $[LaH]_0 = 0.024$ M for $pH_0 = 4.0$ (Fig. 3b). Moreover, the trend of a decreasing shoulder period for increasing $[LaH]_0$ blurred at a pH_0 of ± 3.5. For this value of pH_0, an undissociated lactic acid concentration within the range of 0 to 0.018 M seemed to result in an inactivation curve with a more or less constant shoulder period. Even when $[LaH]_0$ was equal to 0.03 M, the inactivation curve showed the same shoulder length. Overall, for the set of conditions considered, the effect of pH_0 (see Fig. 3, bottom) was much more clear and resulted in a varying shoulder period and inactivation rate.

Similar to the experiments described in the previous section, glucose concentration (data not shown) remained constant during the inactivation process. pH and lactic acid measurements (not shown) sometimes showed an increase during the course of the experiment. For 23.3% of the experiments, total lactic acid increased by more than 0.01 M with an increase in pH higher than 0.2 (all had a shoulder period of >380 h). Only one experiment (3.3%) had similarities to the previous category, but had a less high lactic acid increase (0.005 M). A total of 13.3% of the experiments were characterized by constant lactic acid and pH profiles (four experiments with $pH_0 = 3.5$). For 50% of the experiments, the lactic acid concentration remained constant, but pH increased (less than 0.2). These experiments all had a shoulder period shorter than 380 h. Only 10% of the experiments showed a slight lactic acid decrease, while pH increased for a maximum of 0.2.

Variability in the observed inactivation curves. After all the collected inactivation curves were compared, a certain variation became visible: (i) inactivation curves for identical pH_0-$[LaH]_0$ conditions (for experiments performed in duplicate) did not show identical evolution, and (ii) in the vicinity of the growth/no growth interface, the inactivation process seemed to be a rather contradictory process.

The first type of variation is illustrated in Fig. 3 and 4. Almost identical conditions of $[LaH]_0$ and pH_0 in, for example, Fig. 3a and d and 4a did not show identical behaviors of the inactivation curve. Mostly, duplicate experiments showed equal lengths of the shoulder period, but different slopes in the descent phase. Furthermore, this variation seemed to depend on the severity of the pH_0-$[LaH]_0$ conditions as a lower pH_0 and/or a higher concentration of undissociated lactic acid (so more stressful conditions) in Fig. 4b exhibited almost no difference in the inactivation curves.

In Fig. 5, the variation in the vicinity of the growth/no growth interface is portrayed. Almost similar conditions caused a large difference in shoulder length and slope of the descent phase. The less severe conditions did not match the slowest inactivation process. Moreover, (almost) equal pH_0-$[LaH]_0$ conditions in the considered area displayed a totally different inactivation process (e.g., $pH_0 = 4.02$ to 4.04 in Fig. 3d). Another example of the observed variability in the vicinity of the growth/no growth interface is the experiments with $[LaH]_0 = 0.0194$ M and 0.0202 M in Fig. 2.

Because of the observed variability and in order to exclude experimental inconsistencies, the errors on the plate counting and sampling procedures were determined. This, however, indicated that the errors on plate count results were small (0.01 to 0.07) and not dependent on the position in the inactivation curve. The error on the sampling procedure (0.01 to 0.08) was also small and indicated a homogeneous composition of the experimental medium, as expected for shaken cultures.

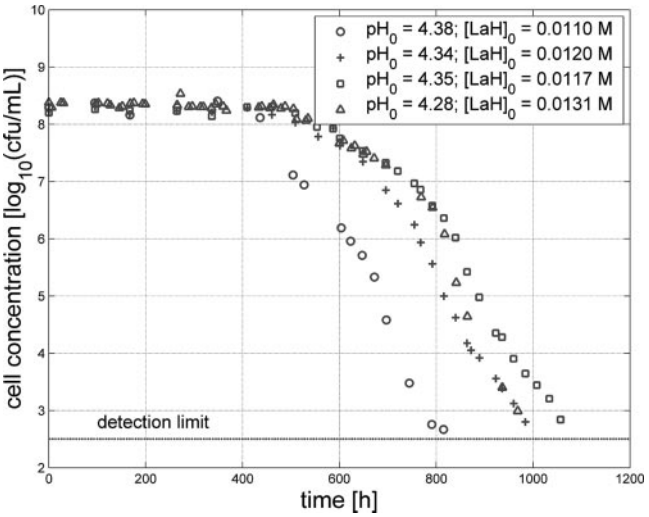

FIG. 5. Variation in inactivation for pH_0-$[LaH]_0$ conditions near the growth/no growth interface.

Microscopic behavior of the *L. innocua* cell during the inactivation process. Microscopic observations of the cell behavior at regular time instances during the inactivation process (for the duplicate experiments) led to the following results. In the beginning of the experiment, and approximately for the length of the shoulder phase, mainly individual cells were observed. In addition, extended cells or long filaments were visible which seemed to show small incisions about one cell length from each other (Fig. 6a). However, when the cell concentration started to decrease, cell aggregates were formed. Cell clumps became clearly visible at a viable cell concentration of 10^5 to 10^6 CFU/ml (Fig. 6b). Only for the experiment with pH_0-$[LaH]_0$ conditions equal to 4.49 for pH_0 and 0.0408 M for $[LaH]_0$ did the cell clumps disintegrate when the viable cell concentration was around the detection limit ($10^{2.5}$ CFU/ml). Thereafter, viable cell concentration increased again (not shown).

The fluorescence microscopy results are summarized in Table 1. Cells were divided into four categories, as proposed by Ben Amor and coworkers (4): (i) cells stained only with cFDA (cF^+ PI^-) contain an intact membrane and functional cytoplasmic enzymes (namely esterases) and were also called viable cells; (ii) the fraction stained with PI only (cF^- PI^+) represents cells with a compromised membrane and were considered dead cells; (iii) cF^+ PI^+ cells, also called injured cells, have functional cytoplasmic enzymes but a partially damaged membrane; and (iv) cF^- PI^- represents the nonviable prelytic cell fraction (12). Observe that a different fourth category was chosen in comparison with reference 4, as the label "lysed cell fraction" did not seem consistent with PI^-. As can be seen, increasing the value of $[LaH]_0$ for an equal pH_0 seemed to result in a higher fraction of viable cells and a lower fraction of dead cells. The cell fractions in the third and fourth categories did not show an obvious trend. As the viable cell concentrations obtained from plate counts for these samples (10^4, 10^5, and 10^6 CFU/ml) were much lower than the viable cell concentrations corresponding to the cF^+ PI^- fraction (10^7, 10^7, and 10^8 CFU/ml, respectively), the viable cell fraction must contain a viable but nonculturable subpopulation.

TABLE 1. Percentage of cells per category for the fluorescence images

$[LaH]_0$ (M)	Mean % of cells (SD)			
	cF^+ PI^-	cF^- PI^+	cF^+ PI^+	cF^- PI^-
0	16.59 (5.50)	53.24 (7.34)	22.21 (6.95)	7.96 (4.97)
0.0400	48.54 (8.01)	16.59 (17.95)	32.19 (14.12)	2.68 (2.16)
0.0610	84.66 (5.06)	4.46 (6.93)	8.88 (4.41)	2.00 (1.93)

Search for the most suitable primary model. All inactivation curves (singular, duplicate, triplicate, or quadruplicate) were taken into account. As described in Materials and Methods, four types of primary inactivation models were calibrated on the experimental data by means of the Microsoft Excel Tool GInaFiT. The results are illustrated for three pH_0-$[LaH]_0$ conditions in Fig. 7. The biphasic model with shoulder (14) was only appropriate for inactivation curves with a concave descent phase preceeded by a short shoulder period in Fig. 7a. For the

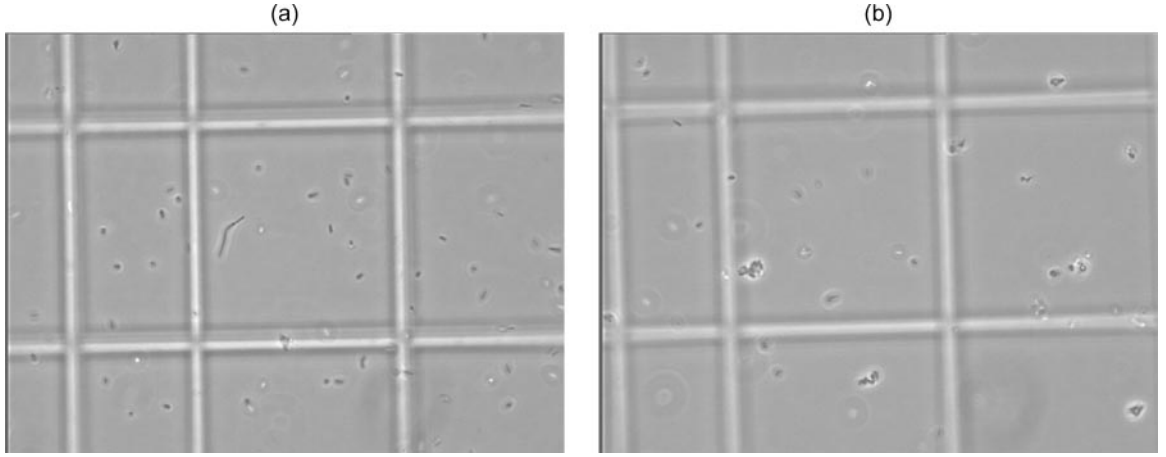

FIG. 6. Microscopic observations of the cell behavior during the inactivation process. (a) Individual cells, extended cells, and long filaments. (b) Cell clumps.

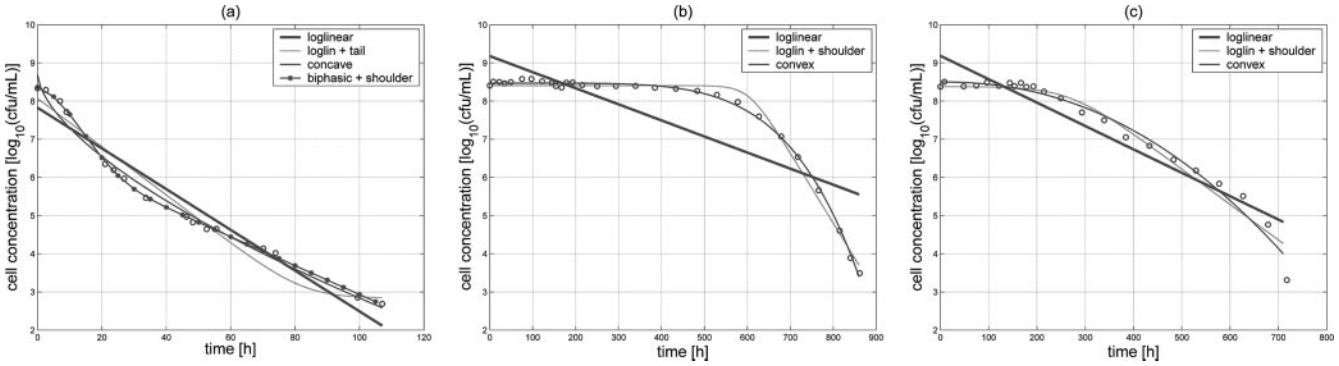

FIG. 7. Description of *L. innocua* inactivation by the four types of inactivation models included in GInaFiT. Inactivation at (a) $pH_0 = 3.49$ and $[LaH]_0 = 0.0504$ M, (b) $pH_0 = 4.37$ and $[LaH]_0 = 0.0153$ M, and (c) $pH_0 = 4.34$ and $[LaH]_0 = 0.0269$ M.

other cases, the model more or less coincided with the log-linear model with a shoulder (13) and is therefore not shown in Fig. 7b and c. For a shoulder with a rounded transition to the descent phase, the convex Weibull-type model (24) seemed to be slightly better than the log-linear model with a shoulder (13). For the curves showing a biphasic descent phase with a slower first phase and faster second phase (see Fig. 7c), the biphasic model was not suitable, and the log-linear model with shoulder and the convex Weibull-type model gave a similar description. The goodness-of-fit data of the calibrated models were compared using the calculated value of the RMSE. For most of the experimental data, either the log-linear model with shoulder or the Weibull-type model gave the best result (high R^2_{adj} and reasonably low RMSE) with the frequency of "most suitable model" for both being about 50%. As there was no preference for one model or the other based on the goodness-of-fit criterion, other factors were to be taken into account. From Fig. 2 and 3, one can conclude that the descent phase of the observed inactivation curves takes one of the following shapes: log-linear, convex, concave, or biphasic. Therefore, the model of the Weibull type (equation 1) was preferred in this study.

Secondary model. The individual effects of the (centered and rescaled) initial pH and initial undissociated lactic acid concentration on the inactivation process are reflected by their influence on the primary model parameters of the Weibull-type model, δ and p.

The following equations were calibrated on the ln(δ) and p data, respectively:

$$\ln(\delta) = b_0 + b_1 \cdot pH_0 + b_2 \cdot [LaH]_0 + b_3 \cdot pH_0^2 + b_4 \cdot [LaH]_0^2 \quad (2)$$

$$\begin{aligned} p &= (p_{max} - p_{min}) \cdot \exp\{-\exp[\alpha(pH_{trans} - pH_0)]\} + p_{min} \\ p_{min} &= c + d \cdot pH_0 + g \cdot pH_0 \cdot [LaH]_0 \\ pH_{trans} &= a \cdot [LaH]_0 + b \end{aligned} \quad (3)$$

Partial F tests as described by Neter et al. (28) indicated an interaction term, $[LaH]_0 \cdot pH_0$, for ln(δ) in equation 2 and a term for $[LaH]_0$ for p_{min} in equation 3 to be insignificant. The resulting parameter values for equations 2 and 3 are presented in Table 2. As can be seen, the 95% confidence intervals for the parameters were small in comparison to the parameter values themselves, which means that all parameters took reliable values. Moreover, based on the value of R^2 (or R^2_{adj}), approximately 93 and 84% of the variability in the ln(δ) and p data were explained by, respectively, model equations 2 and 3 together with their optimal parameter values.

Prediction of δ (i.e., the untransformed values) was obtained by taking the antilogarithm of ln(δ) as depicted below.

$$\delta = \exp\left(\ln(\delta) + \frac{1}{2} \cdot \sigma_R^2\right) \quad (4)$$

σ_R^2 was used as a correction term for bias and is equal to the

TABLE 2. Resulting parameter values and their 95% confidence intervals for the calibration of equations 2 and 3 to the ln(δ) and p data, respectively[a]

Parameter	ln(δ) (95% CI)	Parameter	p (95% CI)
b_0	$4.747\ (\pm 2.289 \times 10^{-1})$	p_{max}	$4.129\ (\pm 3.670 \times 10^{-1})$
b_1	$1.102\ (\pm 1.301 \times 10^{-1})$	c	$1.343\ (\pm 1.804 \times 10^{-1})$
b_2	$-9.656 \times 10^{-1}\ (\pm 1.281 \times 10^{-1})$	d	$2.367 \times 10^{-1}\ (\pm 1.848 \times 10^{-1})$
b_3	$-3.059 \times 10^{-1}\ (\pm 1.340 \times 10^{-1})$	g	$2.768 \times 10^{-1}\ (\pm 2.155 \times 10^{-1})$
b_4	$1.715 \times 10^{-1}\ (\pm 1.203 \times 10^{-1})$	a	$1.517\ (\pm 1.674 \times 10^{-1})$
		b	$1.591\ (\pm 2.055 \times 10^{-1})$
SSE	6.909	SSE	10.007
RMSE	0.406	RMSE	0.494
R^2	0.932	R^2	0.853
R^2_{adj}	0.926	R^2_{adj}	0.835

[a] Preliminary tests indicated that a reliable value for the parameter α was difficult to obtain. Therefore, the parameter was kept constant at an intermediary value of 7.44 in equation 3. The 95% confidence intervals (95% CI) are given in parentheses.

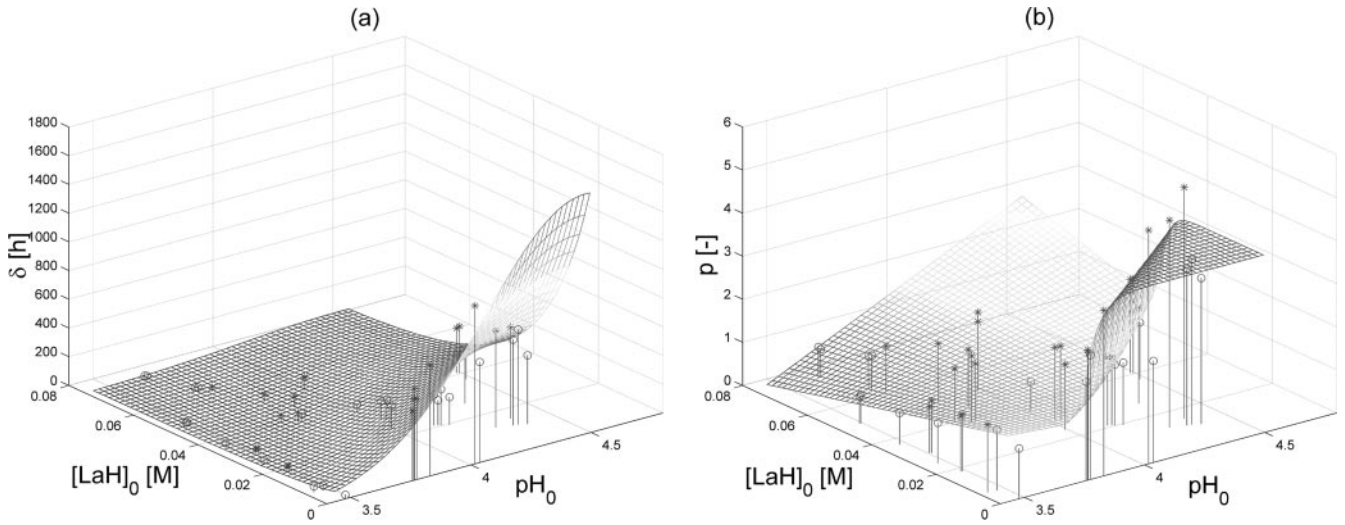

FIG. 8. Simulation of the evolution of δ (a) and p (b) as function of pH_0 and $[LaH]_0$ by means of equations 4 and 3, respectively. Data for δ and p situated above the model surface are indicated by asterisks; data below the surface are indicated by open circles.

sum of squared errors for the regression model to the transformed data divided by the degrees of freedom (26). In Fig. 8, the prediction of δ and p as function of pH_0 and $[LaH]_0$ is graphically presented. To illustrate the application of the developed models in the food industry, the conditions of pH_0 or $[LaH]_0$ necessary to ensure a predetermined inactivation within a predetermined time range can be predicted by the developed models. When one wants to obtain a 2-log reduction ($x = 2$ in Fig. 9) of the microorganism within a time range of 48 h, a total lactic acid concentration of 0.05 M would be necessary in combination with a pH_0 of 3.57 or a total lactic acid concentration of 0.07 M or 0.110 M in combination with a pH_0 of 3.64 and 3.75, respectively. Note that here the conditions are shown with $LaH_{tot,0}$, as this is the method used for practical application. The use of lactic acid in, for example, sprays for carcass decontamination, salad dressings, and feta cheeses can be based on the developed models (18, 23, 29).

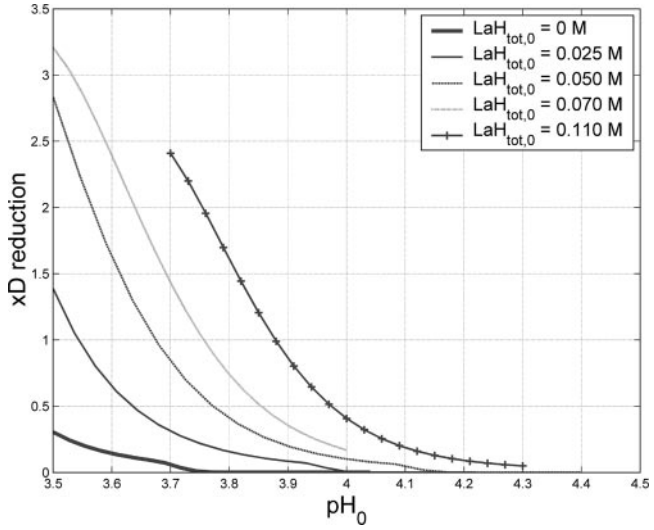

FIG. 9. Prediction of the log reduction (xD reduction) obtained within 48 h for different $LaH_{tot,0}$ concentrations as a function of pH_0.

DISCUSSION

An unusual biphasic inactivation process. Within the experimental results described in this study and illustrated in Fig. 2 to 5, four different shapes of inactivation curves were distinguished: log-linear, convex, concave, and biphasic. These can be interpreted as follows. For the simplest form, the log-linear inactivation, each cell is characterized by an identical sensitivity/resistance to the adverse conditions (i.e., the expected survival times are identical under these adverse conditions). However, due to randomness in lethal hits coming from the environment, not all cells display identical actual survival times and inactivation follows first-order kinetics (11). Convex and concave curve shapes are explained as the existence of a (Weibull-type) distribution of sensitivities within the overall population. In convex curves, surviving cells become more damaged with increasing exposure time and, as such, the inactivation rate increases. For concave curves, on the other hand, first the most sensitive subpopulation is eliminated followed by increasing weakening and, consequently, elimination of the more resistant subpopulation (30). Biphasic behavior is (classically) explained as the existence of two subpopulations within the overall *L. innocua* population, of which the first fraction is more sensitive and the second shows more resistance to the inactivating factor (i.e., the slope of descent phase 1 is higher than the slope of descent phase 2) (10). Nevertheless, for most of the cases of biphasic behavior observed in this study, the second decline phase was steeper than the first one, which is thus in contrast to the (more classic) biphasic inactivation curves such as, for example, that for $[LaH]_0$ equal to 0.036 M in Fig. 3b and those reported in the literature (17, 38, 47).

In contrast, Stumbo (41) presented a curve which can be expected under certain circumstances of thermal treatment and which does show a biphasic behavior with a more steep

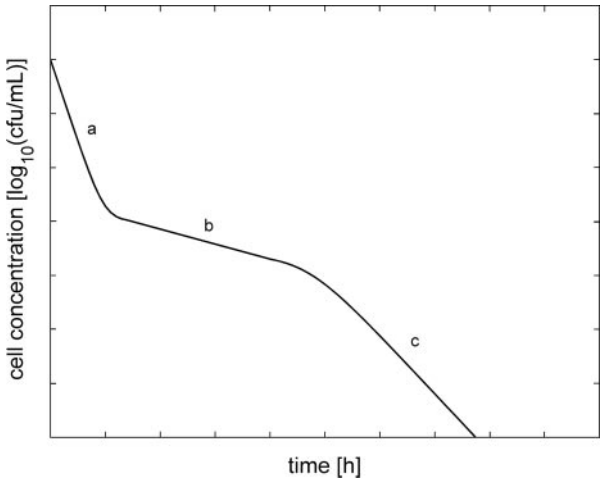

FIG. 10. Inactivation curve to be expected when a flocculation phase occurs during the early phase of the inactivation process (as per Stumbo [41]).

second decline phase. The curve is redrawn in Fig. 10 for clarity. Charles Stumbo explained this unusual biphasic behavior by the existence of cell clumping. In a slow descent phase, the (small) amount of individual cells is inactivated and the number of viable cells per clump is reduced. Then, when each clump contains only one viable cell, a fast descent phase follows which represents the decrease in colony counts originating from one viable cell. The last phases are indicated in Fig. 10 by the symbols b and c, respectively. Thus far, similarity to the biphasic inactivation process observed in our study is possible. However, Stumbo described the existence of a combined flocculation and death phase (a in Fig. 10) before the first slow descent phase during which cell clumps are formed. As a consequence, colony counts (originating from cell clumps now instead of individual cells) decreased. In the present inactivation process, this descent phase was not observed; neither did microscopic observations show cell clumping from the beginning of the experiment on. Cell clumping was observed at a viable cell concentration of approximately 10^6 CFU/ml, which was already in the descent phase.

Another explanation for the observed biphasic behavior is searched for: the biphasic behavior can possibly be interpreted similarly to the phenomenon of convexity. However, in the present study, instead of a continuous increase the inactivation rate showed an abrupt increase caused by a suddenly suffered damage (e.g., a metabolic process that is switched off or an effect that becomes perceptible after some time). An explanation for these effects taking place at different times (at least for some of the pH_0-$[LaH]_0$ conditions tested) must be searched for in the individual effects of both factors. A change in pH_0 affects mainly the exterior environment of the microbial cell and so its behavior (growth, survival, or inactivation). Only in the case of an extreme lowering of the external pH (e.g., 3.5) can a decrease in internal pH be observed (36). The latter can possibly result in a collapse of the pH gradient over the cytoplasmic membrane and, finally, cell death (23, 37). A residing concentration of undissociated lactic acid, on the other hand, influences both its extracellular and cytoplasmic environments. The latter results in a global inhibition through acidification of the cytoplasm and a more specific inhibition of a metabolic function (23). On one hand, a higher value of $[LaH]_0$ (for a fixed pH value) causes more stress to the microorganism as the inactivation proceeds faster (see, for example, other $[LaH]_0$ concentrations in Fig. 3). On the other hand, the fluorescence microscopy data (Table 1) indicate that the fraction of dead cells decreases and the viable cell fraction increases with increasing $[LaH]_0$. In other words, the cell membrane and esterases seem more intact. This can be explained as (i) the fraction of viable but nonculturable cells which strongly increases for increasing $[LaH]_0$ or (ii) an overestimation of the viable cell percentage, as, for example, reported by Breeuwer and Abee (6).

It is imaginable that, depending on the conditions, the pH_0 and $[LaH]_0$ effects occur at distinct moments in the inactivation process, resulting in different (log-linear) parts in the descent phase (see, for example, pH_0 equal to 4.0 and 4.34 in Fig. 3e). In addition, it is possible that for other pH_0-$[LaH]_0$ conditions, the effect of one factor dominates the other, resulting in an inactivation curve with a shape different from biphasic (like log-linear and concave shapes, for example, for pH_0 equal to 3.5 in Fig. 3a). It has to be remarked that the real effect of pH or undissociated lactic acid on the cell metabolism has to be investigated in detail and has not been proven in this study. The changing shape of the inactivation curve is also reflected in the values of the parameter p of the Weibull-type model. Indeed, from Fig. 8b it can be concluded that when conditions become more stressful (i.e., lower pH_0 and/or higher $[LaH]_0$), p decreases from values above 1 (i.e., convex shape), over values equal to 1 (i.e., log-linear inactivation), to values lower than 1 (i.e., concave shape).

Variability on inactivation curves. Increased variance in the bacterial response to less favorable conditions has been widely reported in literature (25, 32). This nonhomogeneous response of microbial populations to stress conditions is explained by differences in cell age, different states in the cell cycle, or variations in the concentrations of transcription factors (8). As described in Materials and Methods, variation in the cell suspension for the experiments with identical pH_0-$[LaH]_0$ conditions (and performed in parallel, see Fig. 1) was circumvented by starting from a mixed inoculum. In spite of that, this does not preclude the occurrence of a minor difference in processes in one of the first stages of the inactivation process, which becomes enlarged as the inactivation proceeds. As indicated above, errors on plate counting and sampling procedures were small and showed a difference in intracellular factors. Other studies reporting results of inactivation experiments performed in replicate often take the mean of the observations to work with (17, 48), which implies the existence of variation, sometimes indicated with error bars. This research indicates that this variation is large in the neighborhood of the growth/no growth interface and shrinks when conditions become more stressful: compare, for example, the inactivation curves for pH_0 equal to ± 4.0 in Fig. 3b, pH_0 set at ± 3.76 in Fig. 3d (both with $[LaH]_0 = 0$ M), and pH_0-$[LaH]_0$ conditions of 3.5 and 0.05 M, respectively, in Fig. 4b.

Concerning the microscopic results for the behavior of the *L. innocua* cell during the inactivation process, the existence of long cell filaments with septa was already observed by other

researchers (5, 15, 49). In addition, in the estimation of the *Listeria* population in a food product under adverse environmental conditions, the observed cell clumping and filament formation might comprise a problem. The viable cell concentration is possibly underestimated, resulting in erroneous conclusions concerning food safety. Also the ability of cell clumps to disintegrate and to start growing again after a certain period under some conditions of pH_0 and $[LaH]_0$ would mean a risk to food safety.

The results presented in this study clearly confirm the existence of distinct, individual effects of an initial pH and initial undissociated lactic acid concentration on the *L. innocua* inactivation. The process was investigated for 30 controlled pH_0-$[LaH]_0$ conditions, and four shapes of inactivation curves could be distinguished. Repeated experiments indicate that the inactivation process is characterized by a certain variability, which seems to be dependent on the severity of the conditions or otherwise stated the distance to the growth/no growth interface. Based on combination of the calibrated primary and secondary models, one can predict which conditions of pH_0 or $[LaH]_0$ are necessary to obtain a predetermined inactivation within a predetermined time range.

ACKNOWLEDGMENTS

This research has been supported by the Fund for Scientific Research—Flanders (FWO) for the postdoctoral fellowship of A.G.; the Belgian Program on Interuniversity Poles of Attraction; and the Second Multiannual Scientific Support Plan for a Sustainable Development Policy, initiated by the Belgian Federal Science Policy Office.

Scientific responsibility is assumed by the authors.

REFERENCES

1. **Abee, T., and J. A. Wouters.** 1999. Microbial stress response in minimal processing. Int. J. Food Microbiol. **50:**65–91.
2. **Albert, I., and P. Mafart.** 2005. A modified Weibull model for bacterial inactivation. Int. J. Food Microbiol. **100:**197–211.
3. **Anonymous.** 2000. Kinetics of microbial inactivation for alternative food processing technologies—IFT's response to Task Order 1, US Food and Drug Administration: how to quantify the destruction kinetics of alternative processing technologies. J. Food Sci. **65**(Suppl.)**:**4–108.
4. **Ben Amor, K., P. Breeuwer, P. Verbaarschot, F. M. Rombouts, A. D. L. Akkermans, W. M. De Vos, and T. Abee.** 2002. Multiparametric flow cytometry and cell sorting for the assessment of viable, injured, and dead bifidobacterium cells during bile salt stress. Appl. Environ. Microbiol. **68:**5209–5216.
5. **Bereksi, N., F. Gavini, T. Bénézech, and C. Faille.** 2002. Growth, morphology and surface properties of *Listeria monocytogenes* Scott A and LO28 under saline and acid environments. J. Appl. Microbiol. **92:**556–565.
6. **Breeuwer, P., and T. Abee.** 2000. Assessment of viability of microorganisms employing fluorescence techniques. Int. J. Food Microbiol. **55:**193–200.
7. **Breidt, F., Jr., J. S. Hayes, and R. F. McFeeters.** 2004. Independent effects of acetic acid and pH on survival of *Escherichia coli* in simulated acidified pickle products. J. Food Prot. **67:**12–18.
8. **Brul, S., F. M. Klis, D. Knorr, T. Abee, and S. Notermans.** 2003. Food preservation and the development of microbial resistance, p. 524–551. *In* P. Zeuthen and L. Bøgh-Sørensen (ed.), Food preservation techniques. CRC Press, Boca Raton, FL.
9. **Buchanan, R. L., M. H. Golden, and R. C. Whiting.** 1993. Differentiation of the effects of pH and lactic or acetic acid concentration on the kinetics of *Listeria monocytogenes* inactivation. J. Food Prot. **56:**474–478, 484.
10. **Cerf, O.** 1977. Tailing of survival curves of bacterial spores. J. Appl. Bacteriol. **42:**1–19.
11. **Cole, M. B., K. W. Davies, G. Munro, C. D. Holyoak, and D. C. Kilsby.** 1993. A vitalistic model to describe the thermal inactivation of *Listeria monocytogenes*. J. Ind. Microbiol. **12:**232–239.
12. **Decker, E.-M.** 2001. The ability of direct fluorescence-based, two-colour assays to detect different physiological states of oral streptococci. Lett. Appl. Microbiol. **33:**188–192.
13. **Geeraerd, A. H., C. H. Herremans, and J. F. Van Impe.** 2000. Structural model requirements to describe microbial inactivation during a mild heat treatment. Int. J. Food Microbiol. **59:**185–209.
14. **Geeraerd, A. H., V. P. Valdramidis, and J. F. Van Impe.** 2005. GInaFiT, a freeware tool to assess non-loglinear microbial survivor curves. Int. J. Food Microbiol. **102:**95–105.
15. **Hazeleger, W. C., M. Dalvoorde, and R. R. Beumer.** 2006. Fluorescence microscopy of NaCl-stressed, elongated *Salmonella* and *Listeria* cells reveals the presence of septa in filaments. Int. J. Food Microbiol. **112:**288–290.
16. **Hill, C., P. D. Cotter, R. D. Sleator, and C. G. M. Gahan.** 2002. Bacterial stress response in *Listeria monocytogenes*: jumping the hurdles imposed by minimal processing. Int. Dairy J. **12:**273–283.
17. **Humpheson, L., M. R. Adams, W. A. Anderson, and M. B. Cole.** 1998. Biphasic thermal inactivation kinetics in *Salmonella enteritidis* PT4. Appl. Environ. Microbiol. **64:**459–464.
18. **ICMSF.** 1998. Microorganisms in foods 6. Microbial ecology of food commodities. Blackie Academic & Professional, London, United Kingdom.
19. **Janssen, M., A. H. Geeraerd, F. Logist, Y. De Visscher, K. M. Vereecken, J. Debevere, F. Devlieghere, and J. F. Van Impe.** 2006. Modelling *Yersinia enterocolitica* inactivation in coculture experiments with *Lactobacillus sakei* as based on pH and lactic acid profiles. Int. J. Food Microbiol. **111:**59–72.
20. **Kelly, A. F., and R. A. Patchett.** 1996. Lactate and acetate production in *Listeria innocua*. Lett. Appl. Microbiol. **23:**125–128.
21. **Le Marc, Y., V. Huchet, C. M. Bourgeois, J. P. Guyonnet, P. Mafart, and D. Thuault.** 2002. Modelling the growth kinetics of *Listeria* as a function of temperature, pH and organic acid concentration. Int. J. Food Microbiol. **73:**219–237.
22. **Leroy, F., K. Lievens, and L. De Vuyst.** 2005. Interactions of meat-associated bacteriocin-producing lactobacilli with *Listeria innocua* under stringent sausage fermentation conditions. J. Food Prot. **68:**2078–2084.
23. **Lund, B. M., and T. Eklund.** 2000. Control of pH and use of organic acids, p. 175–199. *In* B. M. Lund, T. C. Baird-Parker, and G. W. Gould (ed.), The microbiological safety and quality of food, vol. I. Aspen Publishers, Inc., Gaithersburg, MD.
24. **Mafart, P., O. Couvert, S. Gaillard, and I. Leguerinel.** 2002. On calculating sterility in thermal preservation methods: application of the Weibull frequency distribution model. Int. J. Food Microbiol. **72:**107–113.
25. **McClure, P. J., C. de W. Blackburn, M. B. Cole, P. S. Curtis, J. E. Jones, J. D. Legan, I. D. Ogden, M. W. Peck, T. A. Roberts, J. P. Sutherland, and S. J. Walker.** 1994. Modelling the growth, survival and death of microorganisms in foods: the UK Food Micromodel approach. Int. J. Food Microbiol. **23:**265–275.
26. **McMeekin, T. A., J. N. Olley, T. Ross, and D. A. Ratkowsky.** 1993. Predictive microbiology: theory and application. John Wiley and Sons Inc., New York, NY.
27. **McMeekin, T. A., and T. Ross.** 1996. Shelf life prediction: status and future possibilities. Int. J. Food Microbiol. **33:**65–83.
28. **Neter, J., M. H. Kutner, C. J. Nachtsheim, and W. Wasserman.** 1996. Applied linear statistical models. McGraw-Hill, Boston, MA.
29. **Paulsen, P., and F. J. M. Smulders.** 2003. Combining natural antimicrobial systems with other preservation techniques: the case of meat, p. 71–89. *In* P. Zeuthen and L. Bøgh-Sørensen (ed.), Food preservation techniques. CRC Press, Boca Raton, FL.
30. **Peleg, M.** 2000. Microbial survivor curves—the reality of flat "shoulders" and absolute thermal death times. Food Res. Int. **33:**531–538.
31. **Presser, K. A., D. A. Ratkowsky, and T. Ross.** 1997. Modelling the growth rate of *Escherichia coli* as a function of pH and lactic acid concentration. Appl. Environ. Microbiol. **63:**2355–2360.
32. **Ratkowsky, D. A., T. Ross, T. A. McMeekin, and J. Olley.** 1991. Comparison of Arrhenius-type and Bĕlehrádek-type models for prediction of bacterial growth in foods. J. Appl. Bacteriol. **71:**452–459.
33. **Ratkowsky, D. A.** 2004. Model fitting and uncertainty, p. 151–196. *In* R. C. McKellar and X. Lu (ed.), Modeling microbial responses in food. CRC Press, Boca Raton, FL.
34. **Ross, R. P., S. Morgan, and C. Hill.** 2002. Preservation and fermentation: past, present and future. Int. J. Food Microbiol. **79:**3–16.
35. **Russell, J. B.** 1992. Another explanation for the toxicity of fermentation acids at low pH: anion accumulation versus uncoupling. J. Appl. Bacteriol. **73:**363–370.
36. **Shabala, L., B. Budde, T. Ross, H. Siegumfeldt, and T. McMeekin.** 2002. Responses of *Listeria monocytogenes* to acid stress and glucose availability monitored by measurements of intracellular pH and viable counts. Int. J. Food Microbiol. **75:**89–97.
37. **Shabala, L., T. McMeekin, B. B. Budde, and H. Siegumfeldt.** 2006. *Listeria innocua* and *Lactobacillus delbrueckii* subsp. *bulgaricus* employ different strategies to cope with acid stress. Int. J. Food Microbiol. **110:**1–7.
38. **Shadbolt, C. T., T. Ross, and T. A. McMeekin.** 1999. Nonthermal death of *Escherichia coli*. Int. J. Food Microbiol. **49:**129–138.
39. **Siegumfeldt, H., K. B. Rechinger, and M. Jakobsen.** 2000. Dynamic changes of intracellular pH in individual lactic acid bacterium cells in response to a rapid drop in extracellular pH. Appl. Environ. Microbiol. **66:**2330–2335.
40. **Skandamis, P. N., and G.-J. E. Nychas.** 2003. Modeling the microbial interaction and the death of *Escherichia coli* O157:H7 during the fermentation of Spanish-style green table olives. J. Food Prot. **66:**1166–1175.
41. **Stumbo, C. R.** 1973. Thermobacteriology in food processing. Academic Press, Inc., Orlando, FL.
42. **Thylin, I., P. Schuisky, S. Lindgren, and J. C. Gottschal.** 1995. Influence of

pH and lactic acid concentration on *Clostridium tyrobutyricum* during continuous growth in a pH-auxostat. J. Appl. Bacteriol. **79:**663–670.

43. **Van Impe, J. F., B. M. Nicolaï, T. Martens, J. De Baerdemaeker, and J. Vandewalle.** 1992. Dynamic mathematical model to predict microbial growth and inactivation during food processing. Appl. Environ. Microbiol. **58:**2901–2909.
44. **Van Impe, J. F., K. Bernaerts, A. H. Geeraerd, F. Poschet, and K. J. Versyck.** 2001. Modelling and prediction in an uncertain environment, p. 156–179. *In* L. M. M. Tijskens, M. L. A. T. M. Hertog, and B. M. Nicolaï (ed.), Food process modelling. Woodhead Publishing Limited, Cambridge, United Kingdom.
45. **Vereecken, K. M., M. Antwi, M. Janssen, A. Holvoet, F. Devlieghere, J. Debevere, and J. F. Van Impe.** 2002. Biocontrol of microbial pathogens with lactic acid bacteria: evaluation through predictive modelling, p. 163–166. *In* Proceedings & Abstracts of the 18th International ICFMH Symposium, Matforsk. Norwegian Food Research Institute, Matforsk, Norway.
46. **Vereecken, K. M., F. Devlieghere, A. Bockstaele, J. Debevere, and J. F. Van Impe.** 2003. A model for lactic acid induced inhibition of *Yersinia enterocolitica* in mono- and coculture with *Lactobacillus sakei*. Food Microbiol. **20:**701–713.
47. **Virto, R., D. Sanz, I. Álvarez, S. Condon, and J. Raso.** 2004. Relationship between inactivation kinetics of a *Listeria monocytogenes* suspension by chlorine and its chlorine demand. J. Appl. Microbiol. **97:**1281–1288.
48. **Virto, R., D. Sanz, I. Álvarez, S. Condon, and J. Raso.** 2005. Inactivation kinetics of *Yersinia enterocolitica* by citric and lactic acid at different temperatures. Int. J. Food Microbiol. **103:**251–257.
49. **Zaika, L. L., and J. S. Fanelli.** 2003. Growth kinetics and cell morphology of *Listeria monocytogenes* Scott A as affected by temperature, NaCl and EDTA. J. Food Prot. **66:**1208–1215.
50. **Zwietering, M. H., I. Jongenburger, F. M. Rombouts, and K. van 't Riet.** 1990. Modeling of the bacterial growth curve. Appl. Environ. Microbiol. **56:**1875–1881.